

collisional Stark-mixing effect.¹⁹ The cascade time of π^- in hydrogen has been measured²⁰ to be 2.3×10^{-12} sec. The cascade time of antiprotons in hydrogen cannot be measured directly; however, it is very likely shorter because the S -state \bar{p} - p interaction is much stronger than the π^- - p interaction. This means that antiprotons bound to protons will have less chance to transfer than π^- .

To include the possibility of transfer, Eq. (4) should be written

$$W = \frac{A_L}{Z^2} \frac{n}{mZ+n} (1 - P_\pi), \quad (5)$$

where P_π is the probability that the π transfers from the

¹⁹ T. B. Day, G. A. Snow, and J. Sucher, *Phys. Rev. Letters* **3**, 61 (1959); A. S. Wightman, thesis, Princeton University, 1949 (unpublished); M. Leon and H. A. Bethe, *Phys. Rev.* **127**, 636 (1962).

²⁰ T. H. Fields, G. B. Yodh, M. Derrick, and J. G. Fetkovich, *Phys. Rev. Letters* **5**, 69 (1960); J. H. Doede, R. H. Hildebrand, M. H. Israel, *Phys. Rev.* **129**, 2808 (1963); E. Bierman, S. Taylor, E. L. Koller, P. Stamer, and T. Huetter, *Phys. Letters* **4**, 351 (1963).

proton during the cascade. For antiprotons, the same equation applies with P_π replaced with $P_{\bar{p}}$.

If we make the extreme assumption that the transfer probability of \bar{p} stopped in propane is negligible ($P_{\bar{p}}=0$), and that in all other respects π^- and \bar{p} behave alike in their respective atomic and molecular states, our results imply that $A_L=11.7$. This means that, for instance in CH_3 , 8% of π^- are initially bound to protons, and 84% of these are transferred to carbon.²¹ This value of 84% transfer is in the nature of a lower limit because of the assumption that \bar{p} transfer is negligible.

ACKNOWLEDGMENTS

We are indebted to V. Sevcik and the 40-in.-bubble-chamber crew for their efforts in producing good film in the first propane run of that chamber. We gratefully acknowledge the programming assistance of Dr. C. Meltzer and Dr. W. Heintzelman and Frank Sharkey.

²¹ This result is rough in that it assumes that transfer of π^- in all hydrocarbons is equally probable, in Eq. (5).

Study of the Reactions $\pi^- p \rightarrow p \pi^- \text{MM}^0$ and $\pi^- p \rightarrow p \pi^+ \pi^- \pi^- \text{MM}^0$ at 8 GeV/c*

A. R. DZIERBA,[†] W. D. SHEPHARD, N. N. BISWAS, N. M. CASON, P. B. JOHNSON,[‡] V. P. KENNEY, AND J. A. POIRIER

Department of Physics, University of Notre Dame, Notre Dame, Indiana 46556

(Received 3 August 1970)

Results are presented from a hydrogen-bubble-chamber study of the final states $p\pi^- \text{MM}^0$ and $p\pi^+ \pi^- \pi^- \text{MM}^0$, where MM^0 represents a neutral boson state of mass $\geq 2m(\pi^0)$. The proton was identified by ionization for all events in the sample. Production of η^0 , ω^0 , and f^0 mesons with decays into all neutral particles is observed in the $p\pi^- \text{MM}^0$ final state. Peaks are observed in the $\eta^0 \pi^-$ spectrum at 1080 and 1310 MeV. The higher-mass peak has mass 1306 ± 8 MeV and width 41_{-16}^{+20} MeV and is identified as the A_2 . The branching ratio for $A_2 \rightarrow \eta^0 \pi^- / A_2 \rightarrow (\rho \pi)^-$ has been measured as $(18 \pm 7)\%$. There is no evidence for a 980-MeV $\eta^0 \pi^-$ enhancement. Data on the $p\pi^+ \pi^- \pi^- \text{MM}^0$ final state show evidence for η^0 and ω^0 production.

I. INTRODUCTION

THIS paper is one of a series of reports¹⁻¹⁰ on $\pi^- p$ interactions at 8 GeV/c. In this paper we report results¹¹ of a study of the reactions

$$\pi^- p \rightarrow p \pi^- \text{MM}^0 \quad (1)$$

* Work supported in part by the National Science Foundation.

[†] Based upon the dissertation of A.R.D. submitted to the University of Notre Dame in partial fulfillment of requirements for the Ph.D. degree. Present address: Lauritsen Laboratory of High Energy Physics, California Institute of Technology, Pasadena, Calif. 91109.

[‡] Present address: IBM, Owego, N. Y.

¹ I. Derado, J. A. Poirier, N. N. Biswas, N. M. Cason, V. P. Kenney, and W. D. Shephard, *Phys. Letters* **24B**, 112 (1967).

² N. N. Biswas, N. M. Cason, I. Derado, V. P. Kenney, J. A. Poirier, and W. D. Shephard, *Phys. Rev. Letters* **18**, 273 (1967).

³ J. A. Poirier, N. N. Biswas, N. M. Cason, I. Derado, V. P. Kenney, W. D. Shephard, E. H. Synn, H. Yuta, W. Selove, R. Ehrlich, and A. L. Baker, *Phys. Rev.* **163**, 1462 (1967).

⁴ N. N. Biswas, N. M. Cason, P. B. Johnson, V. P. Kenney, J. A. Poirier, and W. D. Shephard, *Phys. Letters* **27B**, 513 (1968).

⁵ N. M. Cason, J. W. Lamsa, N. N. Biswas, I. Derado, T. H.

and

$$\pi^- p \rightarrow p \pi^+ \pi^- \pi^- \text{MM}^0, \quad (2)$$

where MM^0 is a neutral boson state with mass $\geq 2m(\pi^0)$. Thus the final states of these reactions may include

Groves, V. P. Kenney, J. A. Poirier, and W. D. Shephard, *Phys. Rev. Letters* **18**, 880 (1967).

⁶ J. W. Lamsa, N. M. Cason, N. N. Biswas, I. Derado, T. H. Groves, V. P. Kenney, J. A. Poirier, and W. D. Shephard, *Phys. Rev.* **166**, 1395 (1968).

⁷ N. N. Biswas, N. M. Cason, A. R. Dzierba, T. H. Groves, V. P. Kenney, J. A. Poirier, and W. D. Shephard, *Phys. Rev. Letters* **21**, 50 (1968).

⁸ S. J. Barish, W. Selove, N. N. Biswas, N. M. Cason, P. B. Johnson, V. P. Kenney, J. A. Poirier, and W. D. Shephard, *Phys. Rev.* **184**, 1375 (1968).

⁹ N. M. Cason, J. W. Andrews, N. N. Biswas, T. H. Groves, E. A. Harrington, P. B. Johnson, V. P. Kenney, J. A. Poirier, and W. D. Shephard, *Phys. Rev. D* **1**, 851 (1970).

¹⁰ P. H. Stuntebeck, V. P. Kenney, B. J. Deery, N. N. Biswas, N. M. Cason, A. R. Dzierba, M. S. Farber, J. A. Poirier, and W. D. Shephard, *Phys. Letters* **32B**, 391 (1970).

¹¹ Further details are given in A. R. Dzierba, Ph.D. thesis, University of Notre Dame, 1969 (unpublished).

boson resonances with all-neutral decay modes. These reactions are not usually considered in bubble-chamber studies since the presence of more than one neutral particle in the final state precludes kinematic identification of the event. Only events in which the final-state proton was identified by ionization were included. This limits the sample to events in which the laboratory momentum of the proton is less than 1.5 GeV/c.

A bubble-chamber study of this sort was motivated by the success of experiments using the missing-mass-spectrometer (MMS) technique which have reported the discovery of some of the higher-mass boson states¹² as well as the A_2 "splitting."^{13,14} In this technique $M(X^-)$, the effective mass of the mesons recoiling against the proton, is measured by determining the momenta and angles of the incident particle and the final-state proton. An analysis of bubble-chamber data in this fashion can provide further information in that the charged decay products of these meson states, not measured in the MMS experiments, can be detected and measured.

A description of the experimental procedure is given in Sec. II. Reaction (1) is discussed in Sec. III and reaction (2) in Sec. IV.

II. EXPERIMENTAL PROCEDURE

The data for this experiment were obtained from a 42 000 picture exposure in the 80-in. hydrogen bubble chamber at the Brookhaven National Laboratory (BNL). The (8.05 ± 0.04) -GeV/c π^- beam was provided by the BNL dc-separated beam operating in the un-separated mode. A description of the general design considerations for this beam is given elsewhere.^{15,16}

The film was scanned for two- and four-prong events in two separate scans. The events were measured on both film-plane and image-plane measuring projectors. Events with definitely associated Vees were not measured, thus precluding the study of strange-particle production. Events were processed through HGEOM and GRIND.¹⁷ Results of event classification of measured two- and four-prong events are shown in Table I.

Those two- and four-prong events not consistent with

¹² N. M. Focacci, W. Kienzle, B. Levrat, B. Maglic, and M. Martin, Phys. Rev. Letters **17**, 890 (1966). A discussion of the missing-mass-spectrometer techniques is given in B. Maglic and G. Costa, Phys. Letters **18**, 185 (1965).

¹³ G. Chikovani, M. N. Focacci, W. Kienzle, C. Lechanoine, B. Levrat, B. Maglic, M. Martin, P. Schubelin, L. Dubal, M. Fischer, P. Greider, H. A. Neal, and C. Nef, Phys. Letters **25B**, 44 (1967).

¹⁴ Splitting of the A_2 was reported in a bubble-chamber experiment using the missing-mass-spectrometer technique. See D. J. Crennell, U. Karshon, K. W. Lai, J. M. Scarr, and I. O. Skillicorn, Phys. Rev. Letters **20**, 1318 (1968).

¹⁵ I. O. Skillicorn and M. S. Webster, BNL Internal Report No. H-10, 1962 (unpublished).

¹⁶ E. H. Synn, Ph.D. thesis, Physics Department, University of Notre Dame, 1966 (unpublished).

¹⁷ J. W. Burren and J. Sparrow, Rutherford High Energy Laboratory Report No. N1RL/R/14, 1963 (unpublished); R. Böck, CERN Internal Report No. DD/EXP/62/10, 1962 (unpublished); CERN TC Program Library (unpublished).

TABLE I. Event classification of the measured two- and four-prong events.

Final state	Ref. ^a	No. of events ^b	Cross section (mb)
All two-prong events	...	17 800	13.05 ± 0.05
$p\pi^-$	16	3 871	4.9 ± 0.2 ^c
$p\pi^-\pi^0$	8	655	0.48 ± 0.04
$n\pi^+\pi^-$	3,8	1 321	0.90 ± 0.04
All four-prong events	...	16 333	9.96 ± 0.07
$p\pi^+\pi^-\pi^-$	6	1 973	1.27 ± 0.07
$p\pi^+\pi^-\pi^-\pi^0$	9	1 971	1.39 ± 0.09
$n\pi^+\pi^+\pi^-\pi^-$	9	784	0.53 ± 0.04

^a The references quoted give details of the criteria used in selecting events of a particular reaction.

^b The numbers correspond to events in samples satisfying the various measurement and selection criteria.

^c This elastic cross section was estimated by interpolation between π^-p elastic cross-section value tabulated in G. Giacomelli *et al.*, CERN/HERA 69-1 (unpublished).

the specific reactions listed in Table I were considered as candidates for reactions (1) and (2). These candidates were examined on the scanning table and events were selected in which the proton could be definitely identified by ionization. In order to measure the efficiency of this event-identification method, 350 events previously identified⁸ as the reaction

$$\pi^-p \rightarrow p\pi^-\pi^0 \quad (3)$$

were randomly included in the sample of events to be viewed on the scanning table. All of these events included a proton of momentum less than 1.5 GeV/c. Of this subsample, 349 events were identified as having a proton in the final state. In the final sample of identified events, 95% of the protons had a calculated ionization of more than twice the corresponding pion ionization, thus making good discrimination possible for a high percentage of the events.

III. REACTION $\pi^-p \rightarrow p\pi^-MM^0$

A. Introduction

Of the 18 000 measured two-prong events, 2542 events were classified as belonging to the reaction

$$\pi^-p \rightarrow pX^- \quad (1)$$

\searrow
 π^-MM^0

after requiring that (a) the event did not kinematically fit a hypothesis corresponding to elastic scattering or production of a single π^0 , (b) the proton was identified by ionization, and (c) the neutral missing boson mass MM^0 satisfied the condition $MM^0 \geq 2m(\pi^0)$.

The dominant features of reaction (1) are shown in the MM^0 spectrum of Fig. 1 and the $M(X^-)$ spectrum of Fig. 2. Evidence for production of resonances in both of these spectra is presented in the following sections.

B. Neutral-Missing-Mass Spectrum

In order to study possible resonance formation in the MM^0 spectrum, we have made a detailed study of the

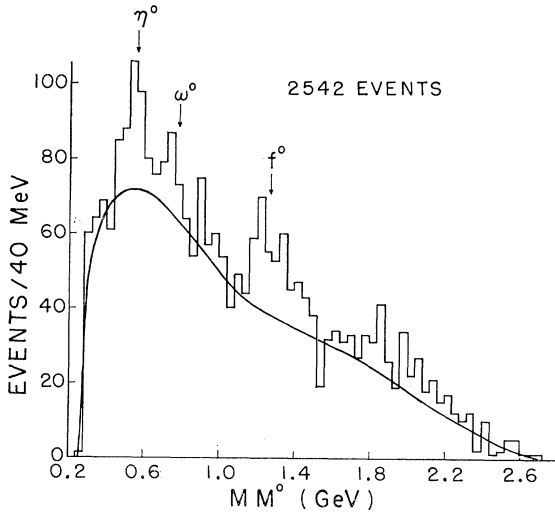
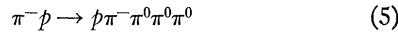


FIG. 1. Distribution of the neutral missing boson mass MM^0 produced in reaction (1). The curve is a Monte Carlo estimate of the $2\pi^0$ and $3\pi^0$ background present in reaction (1). Details are given in the text.

possible backgrounds. Results of this analysis show that the $2\pi^0$ and $3\pi^0$ backgrounds from the reactions



and



provide the dominant contributions. In order to estimate the contributions from these reactions, Monte Carlo events of these types were generated using the program FAKE.¹⁸ In both cases events were generated by requiring that the distribution of momentum transfer from target proton to final-state proton, t_{pp} , be of the form $\exp(-4.5|t_{pp}|)$, to agree with the maximum-likelihood fit to the experimental distribution for reac-

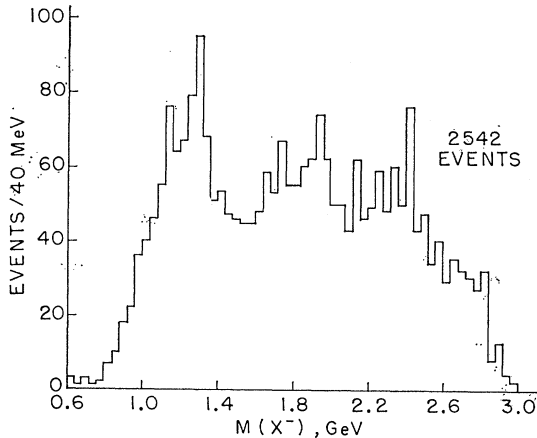
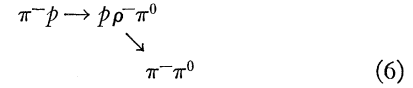


FIG. 2. Distribution of the effective mass of X^- , the boson mass recoiling against the proton in reaction (1).

¹⁸ G. R. Lynch, LRL Report No. UCRL-10335, 1962 (unpublished).

tion (1) shown in Fig. 3. The large enhancement in the 1100–1400-MeV region of the $M(X^-)$ distribution was also taken into account in the final estimate of the $2\pi^0$ contribution. This was accomplished by assuming that the low-mass X^- enhancement decayed primarily into $\rho^-\pi^0$. (Justification for this assumption will be given in Sec. III C.) Therefore, Monte Carlo events of the type



were generated using the same peripherality, and the shape of the $2\pi^0$ spectrum was obtained after constraining the $\pi^-\pi^0\pi^0$ mass to lie in the 1100–1400-MeV mass region. This $2\pi^0$ distribution was then combined with the $2\pi^0$ distribution from reaction (4) in a 1:3 ratio. This ratio represents an estimate of the excess of events above a hand-drawn background in the 1100–1400-MeV mass region of the $M(X^-)$ spectrum. Finally,

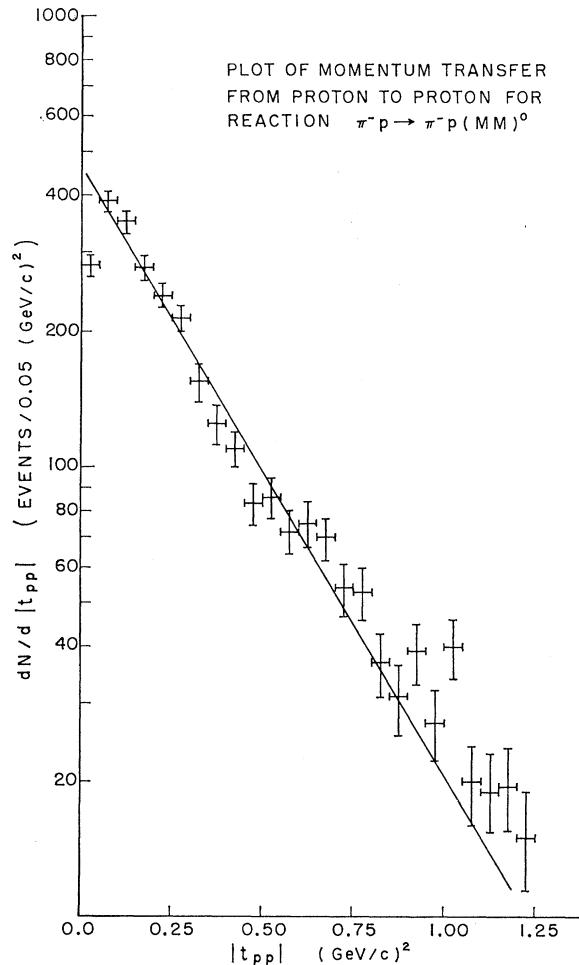


FIG. 3. Distribution of the momentum transfer t_{pp} from target proton to final-state proton in reaction (1). The straight line represents the results of a maximum-likelihood fit to this distribution of the function $N_0 A \exp(-A|t_{pp}|)$, with $A = 4.5$ (GeV/c)⁻².

this resultant $2\pi^0$ contribution was combined with the $3\pi^0$ contribution. The best estimate of the background was obtained when these contributions were added in a 3.25:1 ratio. The tails of the MM^0 spectra for elastic and single- π^0 events which failed the fitting criteria were included in the background.¹¹ The ratio of this contribution to the multi- π^0 background was found to be 1:9.

The final background curve is included in Fig. 4. The missing-mass spectrum shows an excess of events above background at the masses of the η^0 , ω^0 , and f^0 resonances. The estimated production cross sections for these boson states in reaction (1) are given in Table II together with observed cross sections for production of these states with charged decays. The branching ratios are consistent with accepted values. The observed width of the η^0 is consistent with the mass resolution of 94 MeV calculated for this mass region for reaction (1).

C. $\eta^0\pi^-$ Mass Spectrum

In order to search for $\eta^0\pi^-$ resonances we have studied the X^- mass spectrum for MM^0 intervals below, within, and above the η^0 mass interval ($450 \leq MM^0 \leq 650$ MeV). These distributions are shown in Fig. 4. The low-mass enhancements seen in all three $M(X^-)$ plots (at about 980 MeV for $270 \leq MM^0 \leq 450$ MeV, 1080 MeV for $450 \leq MM^0 \leq 650$ MeV, and 1200 MeV for $650 \leq MM^0 \leq 850$ MeV) warrant discussion.

There have been reports of a 980-MeV enhancement produced in KN interactions with an $\eta^0\pi^-$ decay mode.¹⁹ The $M(\eta^0\pi^-)$ spectrum of Fig. 4(b) clearly shows no 980-MeV peak produced in this reaction. A more recent analysis has shown that the 980-MeV $\eta^0\pi^-$ enhancement in KN interactions can be explained as a kinematic effect arising from the presence of the $\Lambda\rho^-\pi^0$ final state.²⁰ In the case of the enhancement in the 980-MeV region in Fig. 4(a), MM^0 lies in the 270–450-MeV interval, corresponding to no known neutral boson.

TABLE II. Cross sections for the production of neutral meson states observed in reaction (1).

	$p\eta^0\pi^-$	$p\omega^0\pi^-$	$pf^0\pi^-$
No. of events	107 \pm 28	42 \pm 23	86 \pm 17
σ (all-neutral decay) μ b	49 \pm 13	19 \pm 11	39 \pm 7
σ (charged decay) ^a μ b	15 \pm 4	180 \pm 20	88 \pm 18
σ (all-neutral)	3.3 ± 1.2	0.11 ± 0.06	0.44 ± 0.12
σ (charged)			
(all-neutral decay)	2.5 ± 0.3	0.11 ± 0.02	0.33
(charged decay) ^b accepted			

^a References 6 and 9.

^b A. Barbaro-Galiteri *et al.*, Rev. Mod. Phys. 42, 87 (1970).

¹⁹ R. Ammar, R. Davis, W. Kropac, J. Mott, D. Salte, B. Werner, M. Derrick, T. Fields, and F. Schweingruber, Phys. Rev. Letters 21, 1832 (1968); D. H. Miller, S. L. Kramer, D. D. Carmony, R. L. Eisner, A. F. Garfinkel, L. J. Gutay, and W. L. Yen, Phys. Letters 29B, 255 (1969).

²⁰ D. J. Crennell, U. Karshon, K. W. Lai, J. S. O'Neill, J. M. Scarr, P. Baumel, R. M. Lea, T. G. Schumann, and E. M. Urvater, Phys. Rev. Letters 22, 1398 (1969).

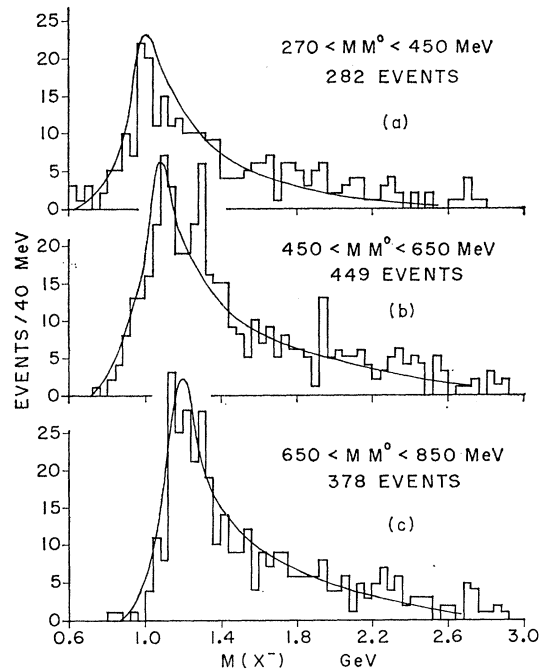


FIG. 4. Distributions of the X^- effective mass for events of reaction (1) with MM^0 in the interval (a) $270 \leq MM^0 \leq 450$ MeV, (b) $450 \leq MM^0 \leq 650$ MeV, and (c) $650 \leq MM^0 \leq 850$ MeV. The curves represent the $\pi^+\pi^-\pi^-$ mass spectrum of reaction (7) for $\pi^-\pi^-$ mass intervals identical to the above MM^0 intervals.

The peak in the 1080-MeV region in the $M(\eta^0\pi^-)$ spectrum [Fig. 4(b)] is not associated with any known $\eta^0\pi^-$ resonance. The apparent mass of this peak is inconsistent with the $\pi_N(1016)$ which has been observed with a $\eta^0\pi^-$ decay mode.²¹ Since the $\eta^0\pi^-$ decay establishes the spin-parity series $J^P=0^+, 1^-, 2^+, \dots$, this peak cannot be identified with the A_1 resonance of mass 1070 MeV for which $J^P=1^+$ is most likely.

We believe that the kinematics of events of the reaction



can account for all of the low-mass enhancements observed in Fig. 4. In order to understand the contribution of these events to the X^- mass spectrum for various $\pi^0\pi^0$ mass intervals, we have studied data of the reaction



from the same experiment.⁶ The final state of reaction (7) is the charged counterpart of reaction (4). Reaction (7) is characterized by the production of large enhancements in the low- 3π -mass region which decay into $\rho^-\pi^-$. From isospin considerations, the decays of these enhancements to $\rho^-\pi^0$ should contribute in equal measure to the X^- spectrum of reaction (1). Indeed although the presence of the ρ^- cannot be directly established, the

²¹ A. Astier, J. Cohen-Ganouna, M. Della Negra, B. Marechal, L. Montanet, M. Tomas, M. Baubillier, and J. Duboc, Phys. Letters 25B, 294 (1967).

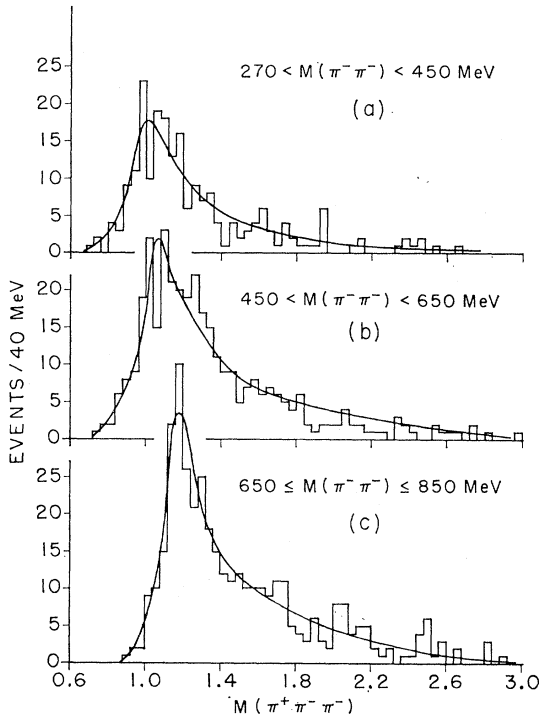


FIG. 5. Distributions of $\pi^+\pi^-\pi^-$ effective mass for events of reaction (7) with $\pi^-\pi^-$ effective mass in the interval (a) $270 \leq M(\pi^-\pi^-) \leq 450$ MeV, (b) $450 \leq M(\pi^-\pi^-) \leq 650$ MeV, and (c) $650 \leq M(\pi^-\pi^-) \leq 850$ MeV. The smooth curves are hand-drawn representations of the distributions.

over-all X^- mass spectrum for this reaction (see Fig. 2) shows a large enhancement in the 1100–1400-MeV mass region consistent in magnitude with the enhancement in the 1100–1400-MeV region of the $\pi^+\pi^-\pi^-$ spectrum in reaction (7). We therefore have plotted the $\pi^+\pi^-\pi^-$ spectrum of reaction (7) for $\pi^-\pi^-$ mass intervals

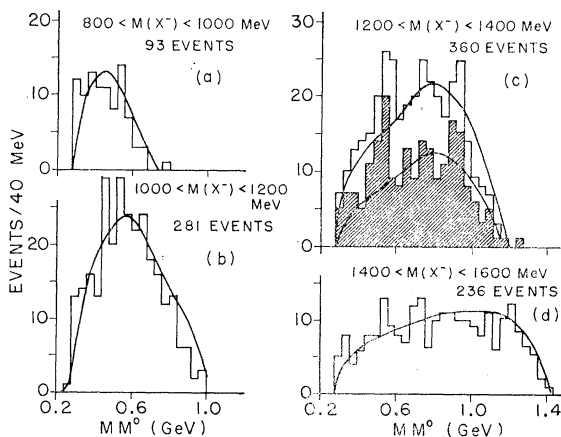


FIG. 6. Distribution of MM^0 for events of reaction (1) in the interval (a) $800 \leq M(X^-) \leq 1000$ MeV, (b) $1000 \leq M(X^-) \leq 1200$ MeV, (c) $1200 \leq M(X^-) \leq 1400$ MeV [shaded events correspond to the interval $1250 \leq M(X^-) \leq 1350$ MeV], and (d) $1400 \leq M(X^-) \leq 1600$ MeV. The curves, obtained from Monte Carlo events, are an estimate of the $2\pi^0$ background.

identical to the MM^0 intervals chosen for Fig. 4. These distributions are shown in Fig. 5 together with smooth curves consistent with them. (We have chosen the $\pi^-\pi^-$ pair so that in both cases the $\pi\pi$ combination on which cuts are made cannot come from the decay of the ρ .) The same curves are shown in Fig. 4 and adequately describe the low-mass enhancements in all three X^- mass spectra. The position of the $\pi^+\pi^-\pi^-$ peak is found to shift smoothly with the $\pi^-\pi^-$ mass cut, in good agreement with the shift of the X^- peak. Thus we believe that all the observed low-mass X^- enhancements are kinematic effects²² resulting from the $p\rho^-\pi^0$ final state when cuts are made on the $\pi^0\pi^0$ mass.

A second peak in the $M(\eta^0\pi^-)$ spectrum of Fig. 4(b) is seen near the A_2 mass. This peak cannot be explained in the same manner as the low-mass enhancements of Fig. 4. The $\eta^0\pi^-$ decay mode of the A_2 has been observed previously in similar π^-p experiments at 5 and 6 GeV/c incident momenta^{14,23} and in a π^+p experiment²⁴ at 7 GeV/c. To determine whether this peak near 1300 MeV is a real $\eta^0\pi^-$ enhancement, we have studied the MM^0 spectrum as a function of $M(X^-)$ as shown in Fig. 6. The curves represent background estimates from Monte Carlo events of reactions (4) and (6). We have taken the ratios of $(p\rho\pi): (p\pi\pi\pi)$ final states to be 0.44:1 as observed in reaction (7). The background curves are in good agreement with estimates from mass distributions observed for reaction (7). The η^0 signal is enhanced for the cut $1200 \leq M(X^-) \leq 1400$ MeV as shown in Fig. 6(c). No such η^0 enhancement is observed for $M(X^-)$ intervals including the 980- or 1080-MeV regions for $M(X^-)$. This supports the interpretation of the 1300-MeV peak as an $\eta^0\pi^-$ effect and further supports the conclusion that no $\eta^0\pi^-$ resonances at 980 or 1080 MeV are observed in this reaction.

D. Production of A_2 in $\eta^0\pi^-$ Channel

In order to determine the parameters of the 1300-MeV enhancement in the A_2 region, we have also considered the charged decay of the η^0 . The η^0 is seen in the $\pi^+\pi^-\pi^0$ mass spectrum of the reaction⁹

$$\pi^-p \rightarrow p\pi^+\pi^-\pi^0. \quad (8)$$

The 29 events consistent with charged decay of the η^0 observed in reaction (8) were added to the $\eta^0\pi^-$ mass spectrum of Fig. 4(b). The resultant distribution is shown in Fig. 7 along with the $\eta^0\pi^-$ mass spectrum of reaction (8) (shaded events). The curve shown is a

²² Since the 680–880-MeV interval for MM^0 includes the ω^0 mass, we have considered the possibility that the broad enhancement centered at ~ 1200 MeV in Fig. 4(c) includes B^- production. From the cross section for B^- production observed in the reaction $\pi^-p \rightarrow p\pi^+\pi^-\pi^0$ at this energy (see Ref. 9), this contribution is expected to be negligible.

²³ G. Ascoli, H. B. Crowley, D. W. Mortara, A. Shapiro, C. A. Bridges, B. I. Eisenstein, U. E. Kruse, E. D. Shafter, and B. Terreault, Phys. Rev. Letters 20, 1321 (1968).

²⁴ A. Barbaro-Galtieri *et al.*, talk presented at the Conference on Experimental Meson Spectroscopy, Philadelphia, 1970 (unpublished).

result of a maximum-likelihood fit of the form

$$\frac{dN}{dM} = B(M) \left[1 + \frac{\frac{1}{2}A\Gamma}{(M-M_r)^2 + \frac{1}{4}\Gamma^2} \right]. \quad (9)$$

The function $B(M)$ represents the background estimate shown in Fig. 4(b). The parameter A specifies the Breit-Wigner contribution. The best fit²⁵ yielded a mass value $M_r = 1306 \pm 8$ MeV, a width $\Gamma = 41_{-16}^{+20}$ MeV, and 32 ± 9 events in the resonance peak. The mass resolution in this region has been calculated to be 15 MeV.²⁶ These values may be compared with the values $M = 1299 \pm 14$ MeV, $\Gamma = 84_{-20}^{+30}$ MeV for $A_2 \rightarrow \rho^0 \pi^-$ observed in the same experiment.⁶

Other experiments have provided information on the $\eta\pi$ decay mode of the A_2 . Ascoli *et al.*²³ observe the decay as a peak in the $\eta^0 \pi^-$ spectrum consistent with the "wide" $A_2^- \rightarrow \rho\pi$. Crenell *et al.*¹⁴ observe a "split" $A_2^- \rightarrow \eta^0 \pi^-$. A recent experiment²⁴ on A_2^+ produced in 7-GeV/ c π^+p interactions indicated no evidence for splitting of the $A_2^+ \rightarrow \eta^0 \pi^+$. The authors report $M = 1314 \pm 8$ MeV and $\Gamma = 113 \pm 25$ MeV for a fit to a single Breit-Wigner resonance. Preliminary results²⁷ on $A_2^- \rightarrow \eta^0 \pi^-$ at 11 GeV/ c obtained by the CERN Boson Spectrometer group show a split peak centered at about 1300 MeV. Thus there is still considerable controversy about the nature of the A_2 .

The fitted mass for $A_2^- \rightarrow \eta^0 \pi^-$ which we obtain is consistent with the mass obtained for $A_2^- \rightarrow \rho^0 \pi^-$ in this experiment and with the mass quoted above for $A_2^+ \rightarrow \eta^0 \pi^+$ observed²⁴ in π^+p interactions at 7 GeV/ c . The best-fit value for the width is narrower than the width obtained in either of these cases and might suggest the interpretation of this peak as the higher-mass component of the A_2 , the A_2^H . However, such an interpretation would imply the suppression of A_2^L decay into $\eta^0 \pi$, in contradiction to the other experiments quoted. In order to study this question we have tried varying the width of the Breit-Wigner peak and varying the detailed shape of the background to see if acceptable fits can be obtained. We find that variations in the background have little effect on the position of the peak but do affect the width significantly. We obtained best-fit values of Γ as small as 18_{-8}^{+14} MeV. When the

²⁵ We have checked to see that the parameters of the 1310-MeV peak do not exhibit systematic shifts resulting from the use of the unfitted momenta in determining them. Thus the events of reaction (1) were kinematically fitted to the final-state hypothesis $p\eta^0\pi^-$. The 1310-MeV peak was seen to persist with no significant change in position or width.

²⁶ We note that our mass resolution in $M(X^-)$ is better than the resolution in MM^0 since the determination of $M(X^-)$ involves only the momentum of the slow proton and of the beam pion, while the determination of MM^0 also requires a knowledge of the additional final-state π^- of reaction (1). The momentum of this π^- is typically quite high, and the absolute uncertainty in the measurement is large compared to that for the proton. The mass resolution in both $M(X^-)$ and MM^0 improves as the mass increases.

²⁷ W. Kienzle, Invited Paper JC3, Spring Meeting of the American Physical Society in Washington, 1970 (unpublished).

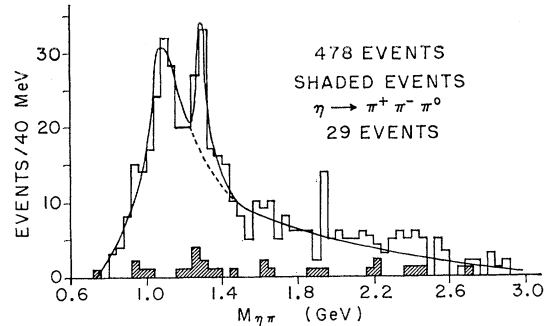


FIG. 7. Distribution of the $\eta^0 \pi^-$ effective mass for the charged (shaded) and neutral decays of the η^0 . The curve is the result of a maximum-likelihood fit to this distribution described in the text.

width was held fixed at 100 MeV an acceptable fit (χ^2 probability $\approx 40\%$) was obtained with a shift in the mass to $M = 1300_{-14}^{+20}$ MeV. Thus we conclude that our results for the mass and width of the A_2 are consistent with those obtained in other experiments.

We have studied the $\eta^0 \pi^-$ mass spectrum in smaller mass intervals and also as a function of the laboratory momentum of the final-state proton in order to duplicate the analysis²⁸ of the groups which have observed A_2 "splitting." Our results for $A_2 \rightarrow \eta^0 \pi^-$ decay show no evidence for a two-peak structure with the statistics available.

We have measured the branching ratio

$$R = (A_2 \rightarrow \eta^0 \pi^-) / [A_2 \rightarrow (\rho\pi)^-]$$

using data on the cross section for $A_2 \rightarrow \rho^0 \pi^-$ from reaction (7) in the same experiment which, from isospin considerations, represents one-half of the cross section for $A_2 \rightarrow (\rho\pi)^-$. We obtain a value²⁹ $R = (18 \pm 7)\%$. For purposes of comparison other values reported for R are $(23 \pm 8)\%$ ²³ at 5 GeV/ c , $(26 \pm 7)\%$ ¹⁴ at 6 GeV/ c , and $(25 \pm 8)\%$ ²⁴ for A_2^+ at 7 GeV/ c .

E. $\eta' \pi^-$ Decay of A_2

We have searched for the $A_2 \rightarrow \eta' \pi^-$ decay observed by Ascoli *et al.*²³ The η' is an $I=0$ pseudoscalar meson of mass 958 MeV. Although the over-all MM^0 spectrum (see Fig. 1) does not show significant production of the η' , there is an excess of events above background in the 958-MeV region of the MM^0 spectrum when the X^- effective mass is constrained to lie in the A_2 mass region. [See Fig. 6(c).] This enhancement is not observed for the other $M(X^-)$ intervals shown in Fig. 6. This suggests that the excess may be due to an $\eta' \pi^-$ decay mode of the A_2 . If we assume that the 8 ± 3 events above

²⁸ Ranges of laboratory momentum and angle for the proton were chosen to duplicate the analysis of Ref. 14 with modifications appropriate for an 8-GeV/ c π^- beam.

²⁹ There is some uncertainty in the $A_2 \rightarrow \eta^0 \pi^-$ cross section since the η^0 also has a $\pi^+ \pi^- \gamma$ decay mode. We have assumed that decays of this type are included with the charged decays added to our sample. The failure of this assumption would correspond to an increase of R to $(19 \pm 7)\%$.

background in the MM^0 spectrum of Fig. 6(c) represent real $\eta'\pi^-$ decays of the A_2 , then it is possible to estimate the branching ratio $R' = (A_2 \rightarrow \eta'\pi^-) / [A_2 \rightarrow (\rho\pi)^-]$. Correcting the number of observed $A_2 \rightarrow \eta'\pi^-$ decays by a factor of 3.7 to account for other decay modes of the η' , we find that R' is $(15 \pm 9)\%$. This ratio is consistent with the value of $(7 \pm 3)\%$ observed by Ascoli *et al.*²³

MacFarlane and Socolow³⁰ have shown that the experimental measurements of the decay rates for members of the 2^+ nonet into members of the 0^- nonet might be used to discriminate between values of the mixing angles corresponding to linear and quadratic mass formulas. The computed branching ratio for $(A_2 \rightarrow \eta'\pi^-) / (A_2 \rightarrow \eta^0\pi^-)$ is 1.08 for the linear mixing angle and 0.21 for the quadratic mixing angle. Thus our result of 0.93 ± 0.43 for this ratio tends to favor the linear mixing angle for the pseudoscalar nonet.

F. Study of $f^0\pi^-$ Mass Spectrum

The data of reaction (7) show evidence for production of the $A_3(1640)$ meson in the $\pi^+\pi^-\pi^-$ effective-mass spectrum for those events with a $\pi^+\pi^-$ effective mass in the f^0 region.⁶ From the production cross section observed for the A_3 in this reaction we expect to see 20 ± 8

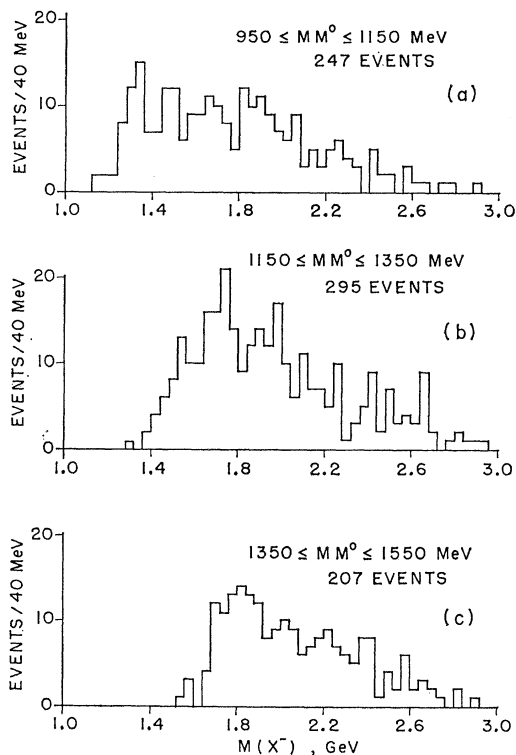
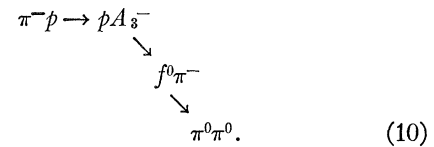


FIG. 8. Distributions of the X^- effective mass for events of reaction (1) with MM^0 in the interval (a) $950 \leq MM^0 \leq 1150$ MeV, (b) $1150 \leq MM^0 \leq 1350$ MeV, and (c) $1350 \leq MM^0 \leq 1550$ MeV.

³⁰ A. J. MacFarlane and R. H. Socolow, *Phys. Rev.* **144**, 1194 (1966).

events of the type



In order to search for this resonance, we have plotted the $M(X^-)$ spectrum for MM^0 intervals below, within, and above the f^0 mass region. These distributions are shown in Fig. 8. There is indication of structure in the X^- effective-mass spectrum for events with MM^0 in the f^0 region [Fig. 8(b)]. However, the observed enhance-

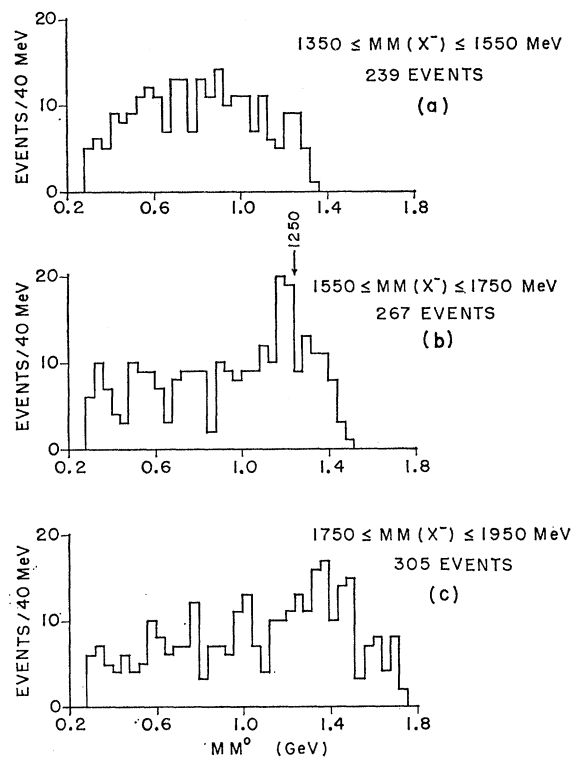


FIG. 9. Distributions of MM^0 for events of reaction (1) with $M(X^-)$ in the interval (a) $1350 \leq M(X^-) \leq 1550$ MeV, (b) $1550 \leq M(X^-) \leq 1750$ MeV, and (c) $1750 \leq M(X^-) \leq 1950$ MeV.

ment is centered at ~ 1700 MeV, a mass somewhat higher than the quoted mass for the A_3 and the mass observed in reaction (7).⁶ The MM^0 spectrum for $M(X^-)$ intervals below, within, and above the quoted A_3 mass interval (1550–1750 MeV) is plotted in Fig. 9. Some enhancement is observed in the f^0 region of the MM^0 spectrum when the X^- effective mass lies in the A_3 region. However, the peak is somewhat below the nominal f^0 mass. This may be due to the fact that the background is falling rapidly just above the 1250-MeV region. The 19 ± 4 events above background in this peak is consistent with the predicted number.

G. Nucleon-Meson System

We have examined the $p\pi^-$ and pMM^0 mass distributions, shown in Fig. 10, for possible baryon-resonance formation. No evidence is seen for any significant baryon-resonance production. An excess in the number of events with masses below 2 GeV may indicate formation of small amounts of several $I_z = \frac{1}{2}$ baryon states and perhaps some $\Delta^0(1236)$ production, but no significant narrow resonance peaks are present. The pMM^0 mass spectrum shows no evidence for significant decay of baryon resonances into $p\pi^0\pi^0$ or $p\pi^0\pi^0\pi^0$. We have also looked for $p\eta^0$ decay modes of baryon resonances by

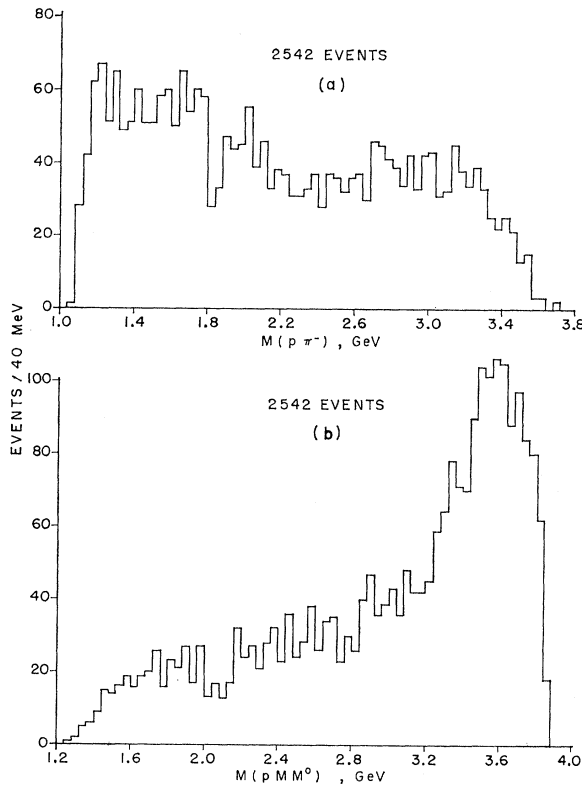


FIG. 10. Distributions of (a) the $p\pi^-$ and (b) pMM^0 effective mass for events of reaction (1).

selecting events with MM^0 in the η^0 mass interval, but observe no significant effects. The lack of evidence for significant $I_z = \frac{1}{2}$ baryon-resonance formation in these data is consistent with what has been observed^{6,9} in reactions (7) and (8).

IV. REACTION $\pi^-p \rightarrow p\pi^+\pi^-\pi^-MM^0$

A. Introduction

Of the 16 000 measured four-prong events, 1067 events were identified as belonging to the reaction

$$\pi^-p \rightarrow p\pi^+\pi^-\pi^-MM^0 \quad (2)$$

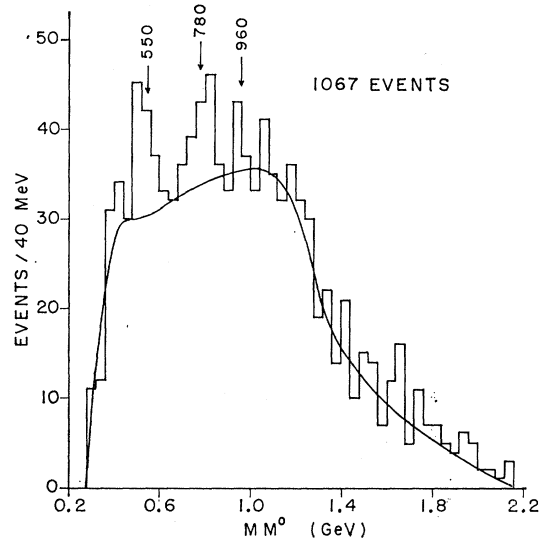


FIG. 11. Distribution of the neutral missing boson mass MM^0 for the 1067 events of reaction (2). The curve is a Monte Carlo estimate of the $2\pi^0$ and $3\pi^0$ background present in reaction (2). Details are given in the text.

after requiring that (a) the reaction did not kinematically fit a hypothesis corresponding to reaction (7) or reaction (8), (b) the proton was identified by ionization, and (c) the neutral missing boson mass MM^0 satisfied the condition $MM^0 > 2m(\pi^0)$.

Since there are three charged pions present in reaction (2) we can study not only the production and decay of resonances with all-neutral decays, but also the production and decay of resonances with charged modes of decay.

B. Neutral Missing Mass

The MM^0 distribution for events of reaction (2) is shown in Fig. 11. In order to understand the shape of this spectrum, we have assumed, as in the two-prong reaction, that our sample is primarily composed of events including two or three π^0 mesons from the reactions

$$\pi^-p \rightarrow p\pi^+\pi^-\pi^-\pi^0\pi^0 \quad (11)$$

and

$$\pi^-p \rightarrow p\pi^+\pi^-\pi^-\pi^0\pi^0\pi^0. \quad (12)$$

The distributions in $2\pi^0$ and $3\pi^0$ effective masses were estimated by generating Monte Carlo events of these types using the program FOWL.³¹ In both cases events were generated by requiring the distribution of momentum transfer from target proton to final-state proton, t_{pp} , to be of the form $\exp(-1.5|t_{pp}|)$, to agree with the observed t_{pp} distribution for reaction (2). The observed t_{pp} distribution is shown in Fig. 12. The relative amounts of $2\pi^0$ and $3\pi^0$ final states were varied to obtain the best agreement between the Monte Carlo

³¹ F. James, CERN Computer 6000 Series Program Library, W505 (unpublished).

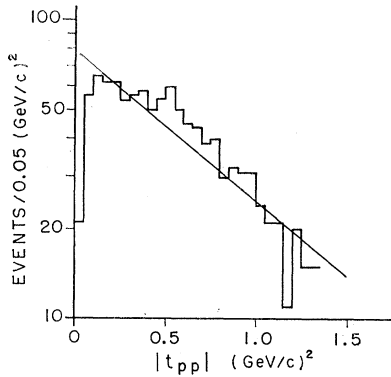


FIG. 12. Distribution of the momentum transfer t_{pp} from target proton to final-state proton for the 1067 events of reaction (2). The straight line represents the result of a maximum-likelihood fit to the distribution of the function $N_0 A \exp(-A|t_{pp}|)$, with $A = 1.5 \text{ (GeV/c)}^{-2}$.

distribution and the MM^0 spectrum. The best agreement was obtained with equal amounts of the $2\pi^0$ and $3\pi^0$ spectra. The resulting background curve is included in Fig. 11. This combination was also found to describe adequately the background in the other effective-mass distributions of reaction (2).

The MM^0 spectrum of reaction (2) shows evidence for the production of the η^0 and ω^0 with all-neutral decay

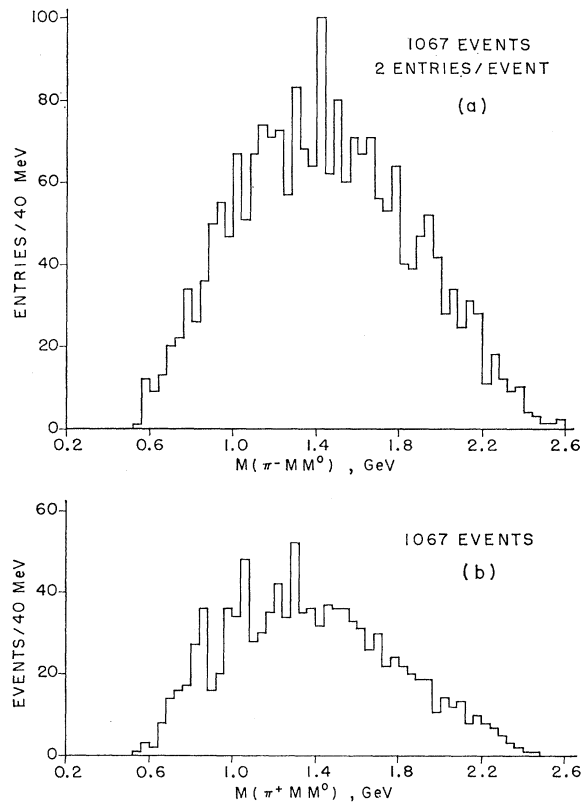


FIG. 13. Distributions of (a) the $\pi^+\pi^-MM^0$ effective mass and (b) the π^+MM^0 effective mass for the 1067 events of reaction (2).

modes. The number of η^0 and ω^0 events observed above background is estimated as 32 ± 16 and 26 ± 19 , respectively, corresponding to production cross sections of 19 ± 10 and $16 \pm 11 \mu\text{b}$.

C. $\pi^\pm MM^0$ Mass Spectra

The over-all π^-MM^0 and π^+MM^0 mass distributions are shown in Fig. 13. Neither spectrum shows evidence for significant decays of resonances into π^\pm plus neutrals. The π^-MM^0 and π^+MM^0 mass spectra for events with the MM^0 below, within, and above the η^0 mass interval were also examined. The structure observed in the $\eta^0\pi^-$ spectrum of the two-prong reaction (1) was not present in either the π^+MM^0 or π^-MM^0 spectra. Adequate descriptions of the distributions for various MM^0 cuts could be obtained by plotting 3π spectra from Monte Carlo events of reaction (11). It was not necessary to include events from reaction (12) since their contribution is negligible for low MM^0 .

The MM^0 distributions for events with the π^-MM^0 effective mass in intervals above, within, and below the

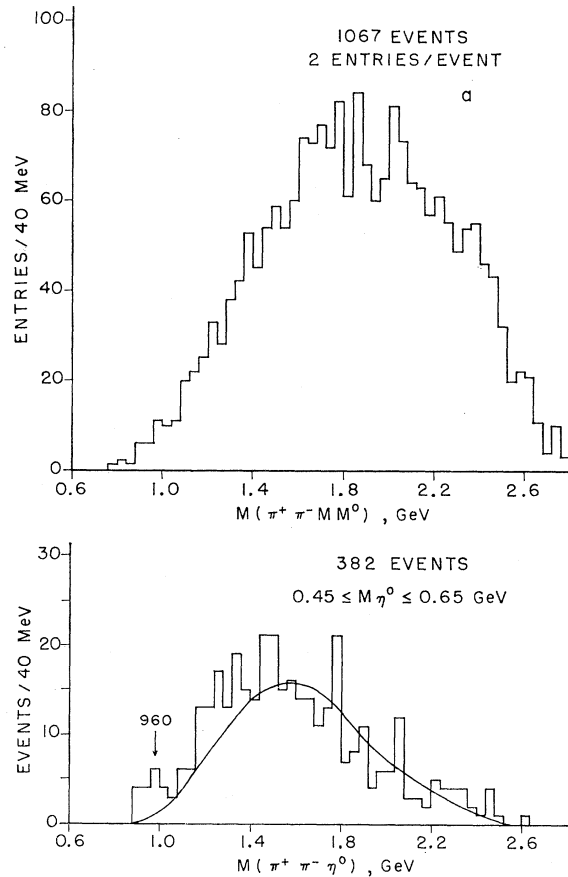


FIG. 14. Distributions of the $\pi^+\pi^-MM^0$ effective mass (a) for the 1067 events of reaction (2) and (b) for the events of reaction (2) with MM^0 in the η^0 mass interval, defined as $0.45 \leq MM^0 \leq 0.65 \text{ GeV}$. The curve is an estimate of the background obtained from Monte Carlo events of reaction (11).

A_2 mass region were examined. No significant signal was observed in the η^0 region for any of these distributions. Thus $A_2 \rightarrow \eta^0 \pi$ is not observed in our sample of $p\pi^+\pi^-\pi^-MM^0$ events.

D. $\pi^-\pi^+MM^0$ and $M(X^-)$ Spectra

The over-all $\pi^+\pi^-MM^0$ spectrum for events of reaction (2) is shown in Fig. 14(a). There is no indication of significant structure in this distribution. There is some indication of structure in the $\pi^+\pi^-MM^0$ mass spectrum of Fig. 14(b) which was obtained by requiring MM^0 to lie in the η^0 interval. The curve shown is a background estimate obtained from Monte Carlo events of reaction (11). There is an excess of events in the low-mass region, indicating possible production of the $\eta'(958)$ with an $\eta^0\pi^+\pi^-$ decay. The number of events above background is estimated as 12 ± 6 , corresponding to a cross section of $7 \pm 4 \mu\text{b}$. After correction for other decay modes of the $\eta'(958)$ and for charged decays of the η^0 , the cross section for $\eta'(958)$ production in reaction (2) is estimated as $23 \pm 13 \mu\text{b}$. This cross section is comparable to the cross section of $50 \pm 20 \mu\text{b}$ reported by Drevermann *et al.*³² for production of $\eta'(958)$ in the reaction $\pi^+p \rightarrow p\pi^+\pi^+\pi^-\pi^-\pi^0$ at 5 GeV/c.

The over-all $M(X^-)$ spectrum, the spectrum of masses recoiling against the proton, has also been examined for possible production of $I=1$ boson resonances decaying into final states of ≥ 4 mesons. No evidence is seen for any resonance production in this distribution.

E. Charged-Particle Mass Spectra

Mass distributions for two or more charged particles from reaction (2) have been examined for the presence of well-known resonances such as the $\rho^0(765)$ and $\Delta^{++}(1236)$ in high-multiplicity final states. The results of our study of reaction (2) may be compared with published studies³²⁻³⁵ of reactions such as

$$\pi^-p \rightarrow p\pi^+\pi^+\pi^-\pi^-\pi^- \quad (13)$$

and

$$\pi^-p \rightarrow p\pi^+\pi^+\pi^-\pi^-\pi^0 \quad (14)$$

in six-prong interactions at incident momenta in the range 5-7 GeV/c. In reaction (2) the multiplicity of combinations for pairs of charged particles is considerably less than it is in six-prong interactions, and one might hope that the reduced background would allow resonance production to be observed more easily. However, in reactions (13) and (14) the only resonances

³² H. Drevermann, U. Idschok, G. Winter, K. Böckmann, A. J. Apostolakis, G. Briggs, C. A. Kitchen, J. V. Major, C. L. Pals, J. Schotanus, D. Toet, R. T. VandeWalle, R. Lestienne, P. Fleury, C. Grosso, B. Quassiatfi, G. Rinaudo, and A. Werbrück, *Phys. Rev.* **161**, 1356 (1967).

³³ F. Bomse, S. Borenstein, E. B. Brucker, A. Callahan, J. Cole, D. Ellis, D. Gillespie, G. Luste, E. Moses, A. Pevsner, and R. Zdanis, *Phys. Rev.* **162**, 1328 (1968).

³⁴ M. A. Ijaz and J. Campbell, *Nucl. Phys.* **B7**, 175 (1968).

³⁵ K. F. Suen, E. D. Alyea, K. F. Galloway, H. J. Martin, Jr., W. E. Powers, and T. M. Small, *Phys. Rev. D* **1**, 54 (1970).

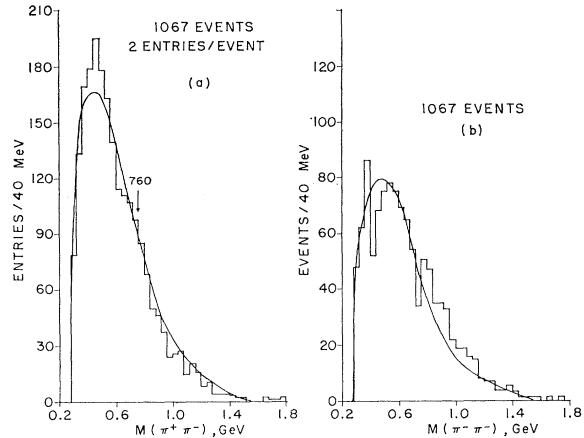


FIG. 15. Distribution of (a) the $\pi^+\pi^-$ effective mass and (b) the $\pi^-\pi^-$ effective mass for the 1067 events of reaction (2). The curves are estimates of the background obtained from Monte Carlo events of reactions (11) and (12).

definitely observed³⁵ in mass distributions for two charged particles have been ρ^0 and $\Delta^{++}(1236)$, both of which involve a π^+ meson. Only one π^+ meson is present in reactions (11) and (12) while there are two π^+ mesons in reactions (13) and (14). In four-prong interactions at comparable energies, less ρ^0 and $\Delta^{++}(1236)$ production is generally seen in π^-p interactions with only one π^+ meson in the final state than in π^+p interactions. We also observe less ρ^0 and $\Delta^{++}(1236)$ production in our data than is reported at 6 GeV/c in reactions (13) and (14).

The $\pi^+\pi^-$ and $\pi^-\pi^-$ spectra for events of reaction (2) are shown in Figs. 15(a) and 15(b), respectively. The curves are estimates of the shape of these spectra obtained from Monte Carlo events of reactions (11) and (12). The $\pi^-\pi^-$ mass distribution is adequately described by the background curve. No significant peaks³⁶ are seen in the $\pi^+\pi^-$ distribution although there may be a slight shoulder in the ρ mass region. Suen *et al.*³⁵ have reported a cross section of $149 \pm 20 \mu\text{b}$ for ρ^0 production in reaction (13) and see no ρ^0 production in reaction (14) at 6 GeV/c. If, as we have estimated, our sample consists primarily of about equal amounts of reactions (11) and (12), a comparable cross section for ρ^0 production in reaction (11) should lead to a significant peak in Fig. 15(a). We conclude that ρ^0 production is significantly less in reaction (11) than in reaction (13) at these energies.

The π^+p and π^-p mass spectra for reaction (2) are shown in Fig. 16. The π^+p mass spectrum shows significant $\Delta^{++}(1236)$ production with a cross section estimated to be $65 \pm 20 \mu\text{b}$. This is to be compared with cross sections for $\Delta^{++}(1236)$ production of 105 ± 15 and $92 \pm 14 \mu\text{b}$ in reactions (13) and (14), respectively, at 6 GeV/c,³⁵ and 250 ± 50 and $350 \pm 50 \mu\text{b}$ in the corre-

³⁶ We believe that the presence of final states involving low-mass mesons such as η^0 and ω^0 is responsible for the excess of events above the background curve in the 500-MeV region of Fig. 15(a).

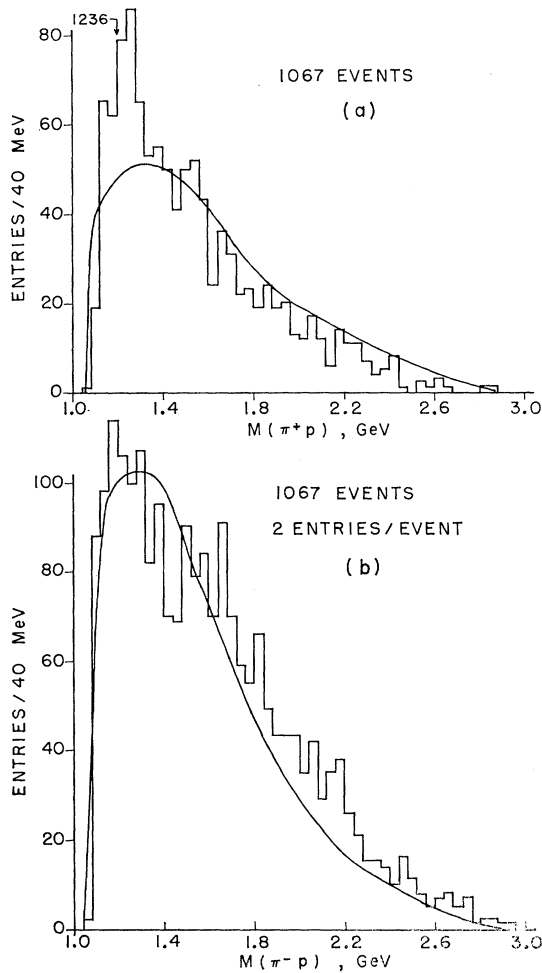


FIG. 16. Distributions of (a) the π^+p effective mass and (b) the π^-p effective mass for the 1067 events of reaction (2). The curves are estimates of the background obtained from Monte Carlo events of reactions (11) and (12).

sponding π^+p reactions at 5 GeV/c.³² Again the observed production of Δ^{++} decreases as the total number of π^+ mesons decreases in final states of comparable multiplicity.

No evidence is seen in Fig. 16(b) for significant production of $I_z = \frac{1}{2}$ isobars. This is consistent with what has been reported³²⁻³⁵ for reactions with six-charged-particle final states.

Suen *et al.*³⁵ have reported production of $A_1^- \rightarrow \rho^0\pi^-$ with a cross section of $51 \pm 9 \mu\text{b}$ in reaction (13) at 6 GeV/c. Our $\pi^+\pi^-\pi^-$ spectrum for events of reaction (2) is shown in Fig. 17, together with a background curve

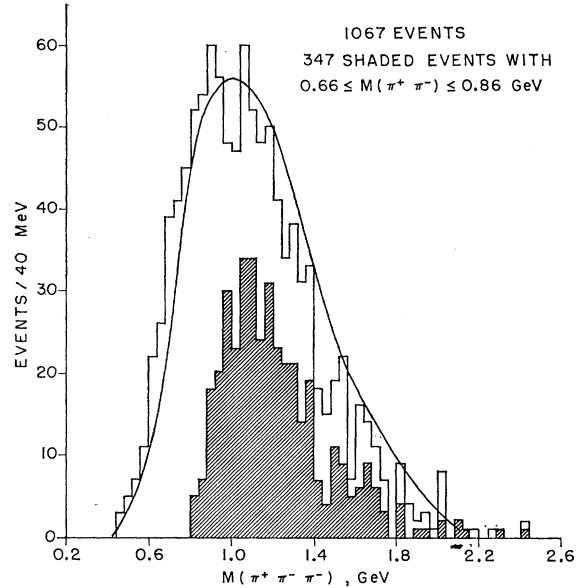


FIG. 17. Distribution of the $\pi^+\pi^-\pi^-$ effective mass for the 1067 events of reaction (2). The shaded events correspond to those events for which the $\pi^+\pi^-$ effective mass is in the ρ mass interval defined by $0.66 \leq M_\rho \leq 0.86$ GeV. The curve is an estimate of the background obtained from Monte Carlo events of reactions (11) and (12).

obtained from Monte Carlo events of reactions (11) and (12). The curve is in fair agreement with the distribution over the entire mass range although there are more events in the low-mass region than predicted by the curve. The $\pi^+\pi^-\pi^-$ distribution for events with $\pi^+\pi^-$ mass in the ρ^0 region is also shown. In both cases the distributions show broad peaks in the mass region near the A_1 mass, but because of uncertainty in the background normalization, it is impossible to attribute this definitely to resonance production. In neither distribution is there evidence for a peak at the A_2 mass.

ACKNOWLEDGMENTS

The help and cooperation of the 80-in.-bubble-chamber group and of the AGS personnel at Brookhaven National Laboratory is gratefully acknowledged. The efforts of all those who helped in the preparation of these data, in particular, Dr. E. H. Synn, Dr. J. W. Andrews, Dr. J. W. Lamsa, and Dr. J. M. Marraffino, were essential to the completion of this study. The work of J. B. Annable in the data analysis is appreciated. We wish to thank our scanning and measuring staff and to acknowledge the cooperation of the Notre Dame Computing Center.